Synthesis of vanadium dioxide thin films and nanoparticles

Synthesis of vanadium dioxide thin films and nanoparticles

Joyeeta Nag and R F Haglund Jr

Department of Physics and Astronomy, Vanderbilt Institute of Nanoscale Science and
Engineering, Vanderbilt University, Nashville, TN 37235-1807, USA

Abstract

Thin-film materials with 'smart' properties that react to temperature variations, electric or
magnetic fields, and/or pressure variations have recently attracted a great deal of attention.
Vanadium dioxide (VO_2) belongs to this family of 'smart materials' because it exhibits a
semiconductor-to-metal first-order phase transition near 340 K, accompanied by an abrupt
change in its resistivity and near-infrared transmission. It is also of great interest in
condensed-matter physics because it is a classic strongly correlated electron system. In order to
integrate vanadium dioxide into microelectronic circuits, thin-film growth of VO_2 has been
studied extensively, and studies of VO_2 nanoparticles have shown that the phase transition is
size-dependent. This paper presents a broad overview of the growth techniques that have been
used to produce thin films and nanoparticles of VO_2, including chemical vapor deposition,
sol–gel synthesis, sputter deposition and pulsed laser deposition. Representative deposition
techniques are described, and typical thin-film characteristics are presented, with an emphasis
on recent results obtained using pulsed laser deposition. The opportunities for growing epitaxial
films of VO_2, and for doping VO_2 films to alter their transition temperature and switching
characteristics, are also discussed.

(Some figures in this article are in colour only in the electronic version)

1. Introduction

Vanadium dioxide has been a hardy perennial in theoretical
and experimental condensed-matter and materials research for
almost half a century (Morin 1959). Bulk vanadium dioxide
crystals exhibit a semiconductor-to-metal transition (SMT),
also widely known as the metal–insulator transition (MIT),
at a critical temperature of about 68 °C, accompanied by a
first-order structural phase transformation from a monoclinic
($P2_1/c$) to tetragonal (rutile—$P4_2/mnm$) structure (Wyckoff
1965), characterized by a small lattice distortion along the c-
axis. As a transition-metal oxide with narrow d-electron bands,
this strongly correlated electron system is extremely sensitive
to small changes in extrinsic parameters such as temperature,
pressure, or doping (Kotliar and Vollhardt 2004, Adler 1968,
Adler and Brooks 1967, Adler *et al* 1967, Berglund and
Guggenheim 1969, Eyert 2002, Liebsch *et al* 2005, Paquet
and Lerouxhugon 1980). The first-order phase transition is
accompanied by an abrupt change in resistivity, as well as
in its near-infrared (IR) optical properties in the 0.8–2.2 μm
region (Barker *et al* 1966, Verleur *et al* 1968). In bulk
crystals, the change in resistivity is of the order of 10^3–10^5,

with a hysteresis width of $\sim$1 °C. In thin films, on the other
hand, hysteresis widths may be of the order of 10–15 °C; in
nanoparticulate VO_2, the hysteresis widths may be even larger.
Figures 1(a) and (b) show hysteresis curves for electrical
resistance and optical reflection, respectively, measured for
typical thin films of VO_2 of order 100 nm thickness.

Experimental and theoretical studies of the SMT
mechanism in bulk VO_2 suggest that it is a mixture of a
pure Mott (electronic) phase transition with a spin-Peierls
lattice instability that reflects the strong correlation. Recent
experiments using femtosecond laser excitation to initiate
the SMT have substantiated this picture in thin films by
time-resolved measurements of the characteristic x-rays,
optical signatures, transient conductivity and coherent phonons
associated with the transition between the two different lattice
structures (Cavalleri *et al* 2004a, 2004b, 2005, 2006, 2001,
Kim *et al* 2006, Kübler *et al* 2007).

Thin films and nanoparticles of VO_2 tend to survive the
stress generated during repeated cycles of phase transition
better than bulk crystals, and also their switching temperature
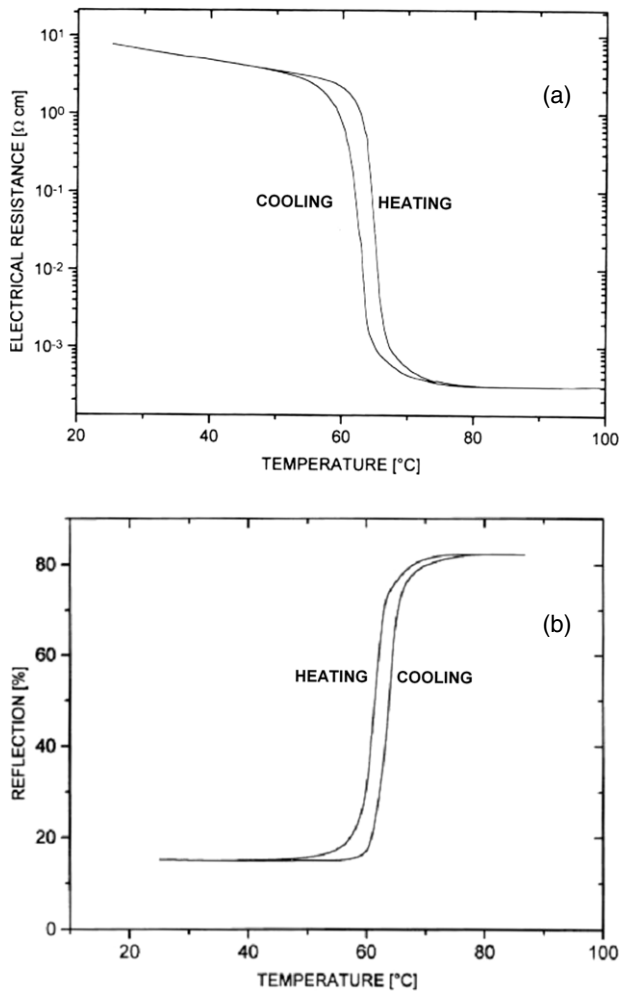can be depressed to near room temperature by doping. Thus

Figure 1. Measured hysteresis curves during the insulator–metal transition of a thin VO$_2$ film for (a) electrical resistance and (b) optical reflectivity at a wavelength of 2.0 μm.

Figure 2. X-ray diffraction (XRD) pattern (θ–2θ scan) for polycrystalline VO$_2$ thin film on Vycor glass with three orders of magnitude resistivity contrast, prepared by chemical vapor deposition (Greenberg 1983). Reprinted with permission from Elsevier (1983).

Figure 3. A Rutherford backscattering (RBS) spectrum for VO$_2$ on silicon, where the ratio of the area under the peaks determines the stoichiometry of the sample. Channel number is proportional to the energy of the backscattered ions.

the metal–insulator transition in VO$_2$ has triggered numerous suggestions for technological applications. These include thermally activated VO$_2$ thin films (Ryabova 1981) and nanoparticles for optical switching and limiting (Becker *et al* 1994, Chen *et al* 2003, Soltani *et al* 2007, 2004b, Lopez *et al* 2004a, Chen *et al* 2004b, Kim *et al* 2004, Walden 1970), thermal relays and energy management devices (Kivaisi and Samiji 1999, Sobhan *et al* 1996, Soltani *et al* 2006, Manning *et al* 2002, Wu *et al* 2000), sensors and actuators (Rajendra Kumar *et al* 2003), electrochromic and photochromic memory and optical devices (Roach 1971, Jorgenson and Lee 1986, Fan *et al* 1977, Chivian *et al* 1985), high-speed solid-state optical displays (Gurvitch *et al* 1999), and a variety of other modulation, polarization, and control functions (Cole *et al* 1998, Radford *et al* 1996, Jerominek *et al* 1993, Duchene *et al* 1972) extending from the near-infrared to the millimeter-wave range (Hood and DeNatale 1991). Applications for VO$_2$ nanoparticles, with their plasmonic response in the vicinity of the near-infrared communications wavelengths (Rini *et al* 2005), ferroelasticity and negative mechanical stiffness (Lakes *et al* 2001), have an even greater range of potential applications that are only beginning to be explored.
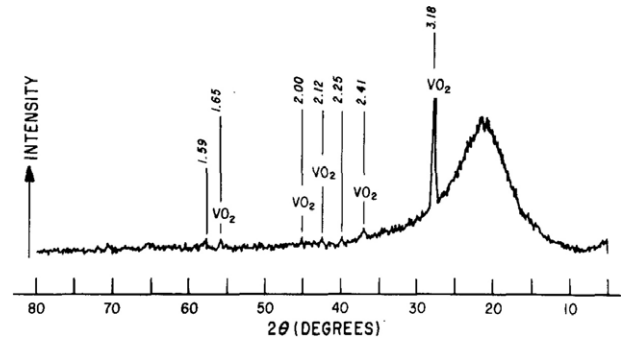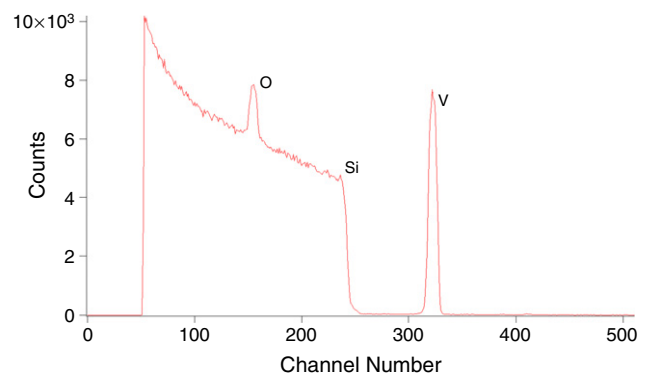
This review deals with the growth of VO$_2$ thin films and nanoparticles, including techniques for growing epitaxial films of VO$_2$, and doping VO$_2$ to alter its transition temperature and switching characteristics (MacChesney and Guggenheim 1969). Nevertheless, this study would be incomplete without a mention of the most widely used characterization techniques (Feldman and Mayer 1986). In general, x-ray diffraction (XRD), Rutherford backscattering (RBS), and Raman spectroscopy are commonly used to determine the stoichiometry and phase of VO$_2$ films and nanoparticles. Figure 2 shows an XRD spectrum of VO$_2$ on Vycor glass, while figure 3 shows an RBS spectrum of VO$_2$ on (100) silicon. Structural characterizations of thin films is primarily done by scanning electron microscopy (SEM), transmission electron microscopy (TEM), atomic force microscopy (AFM), and x-ray photoelectron spectroscopy (XPS). The electrical phase transition properties of VO$_2$ are studied by the four-point probe method to record variations in resistivity with temperature, while the transmission/reflection changes during phase transition are typically observed using a near-IR laser and a detector to measure the transmitted or reflected intensity through the sample, as it is heated or cooled.
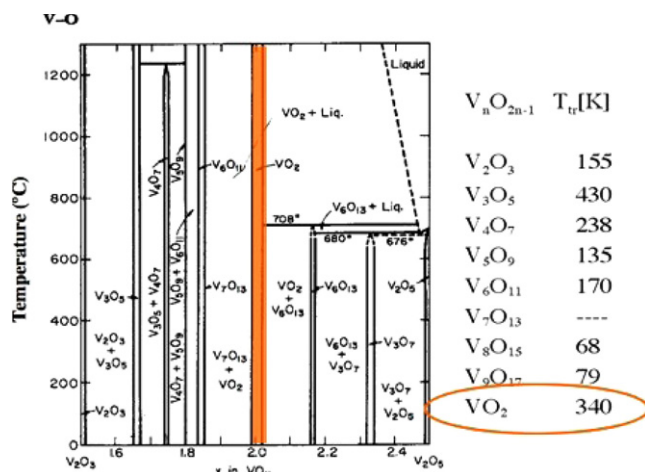
Figure 4. Phase diagram for the vanadium–oxygen system,
(after Griffith and Eastwood 1974).

2. The phase diagram for VO$_2$

In addition to vanadium dioxide (VO$_2$), vanadium sesquioxide
(V$_2$O$_3$) and vanadium pentoxide (V$_2$O$_5$) (T_{tr} = 257 °C)
also exhibit metal–insulator transitions at critical temperatures
specific to their stoichiometric phases. But as the phase
diagram of figure 4 shows, there are nearly 15 to 20 other
stable vanadium oxide phases, such as VO, V$_6$O$_{13}$, V$_7$O$_{13}$
and others that exhibit no metal–insulator transitions. The
existence of these competing oxide phases offers a particular
challenge to the growth of both bulk and thin films of VO$_2$
(Griffith and Eastwood 1974, Schwingenschlogl and Eyert
2004). Nevertheless, stoichiometric VO$_2$ depositions have
been done using techniques as varied as reactive evaporation,
several sputtering methods, metal–organic chemical vapor
deposition (MOCVD), pulsed laser deposition (PLD), and sol–
gel deposition. In this review we will concentrate on the four
techniques most commonly used nowadays for the fabrication
of VO$_2$ thin films and nanoparticles: chemical vapor deposition
(CVD), sol–gel methods sputtering and PLD. But in passing it
should be noted that techniques such as reactive evaporation
have also been extensively employed (Case 1987, 1991, Golan
et al 2003, 2004, Fukuma *et al* 1982, Nyberg and Buhrman
1984) to obtain high-quality VO$_2$ films. Also, vanadium and
oxygen have been co-implanted in the near-surface region of
fused silica (Lopez *et al* 2002a) and alumina (Gea and Boatner
1996, Gea *et al* 1997) substrates at a ratio of 1:2; subsequent
annealing at 1100 °C led to the precipitation of crystalline
nanoparticles with reasonably narrow size distributions. The
ion-implanted samples were used in the discovery of size-
dependent effects, including greatly enhanced hysteresis, in the
structural phase transition of VO$_2$ nanoparticles (Lopez *et al*
2001, 2002b, 2004c).

3. Chemical vapor deposition

Chemical vapor deposition (CVD) is a common industrial
process for depositing high-quality and high-performance thin
films. In a typical CVD process, the wafer (substrate) is

exposed to one or more volatile precursors, which react
and/or decompose on the substrate surface to produce the
desired deposit. Frequently, volatile byproducts are also
produced, which are removed by gas flow through the reaction
chamber. In the case of VO$_2$, the process is almost always
based on organometallic precursors, and is therefore often
called organometallic chemical vapor deposition (OMCVD) or
metal–organic chemical vapor deposition (MOCVD).

The first deposition technique used for the deposition of
VO$_2$ thin films appears to have been CVD, and after half a
century it is still used extensively. Koide and Takei, who in
1966 had grown bulk single crystals of VO$_2$ by CVD (Takei
and Koide 1966), grew thin films of VO$_2$ a year later by
the same method (Koide and Takei 1967). They introduced
fumes of vanadium oxychloride (VOCl$_3$) carried by N$_2$ gas
into the growth chamber, which was then hydrolyzed on the
surface of rutile substrates to give epitaxial VO$_2$ films. In
1968, MacChesney, Potter, and Guggenheim (MacChesney
et al 1968) used CO$_2$ rather than N$_2$ to transport VOCl$_3$,
and V$_2$O$_5$ was formed on single-crystal sapphire substrates.
This V$_2$O$_5$ was then reduced to VO$_2$ by annealing between
500° and 550 °C, with appropriate oxygen partial pressures,
in a controlled atmosphere containing a mixture of CO and
CO$_2$. These same researchers were the first to elucidate
the phase diagram for the vanadium–oxygen system. Thin-
film VO$_2$ preparation on various substrates by the pyrolysis
of vanadium acetylacetonate (C$_5$H$_7$O$_2$)$_4$V in a controlled
atmosphere with appropriate mixtures of nitrogen and oxygen
was accomplished in 1972 by a Russian group (Ryabova *et al*
1972).

$$(C_5H_7O_2)_4V \xrightarrow{\text{heat}} VO_x + \text{gases.} \qquad (1)$$
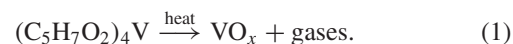
Composition of the gas carrier was found to be the principal
determinant of film composition. Vanadyl tri-isopropoxide
(VO(OC$_3$H$_7$)$_3$)-based CVD was first tried in open atmosphere
in 1983 (Greenberg 1983, 1994), and VO$_2$ films were
successfully deposited on glass with and without post-
annealing.

CVD continues to be one of the most convenient ways
of making VO$_2$, using any one of the above precursor
formulations. Even VCl$_4$ and water as precursors have been
used by Manning *et al* (2002) to make intelligent window
coatings with VO$_2$. Maruyama and Ikuta (1993) demonstrated
atmospheric-pressure CVD (APCVD) from vanadium (III)
acetylacetonate, to deposit polycrystalline VO$_2$ films on fused
quartz and sapphire single crystals. Manning *et al* (Manning
and Parkin 2004a, 2004b, Manning *et al* 2005) have also
investigated APCVD in quite extensive detail for various
purposes, and have successfully demonstrated doping of VO$_2$
with W, Ti, Mo, and Nb. High-quality epitaxial VO$_2$ films
were grown on sapphire substrates using low-pressure CVD
by Zhang *et al* (1994), and the substrate and film orientations
were characterized. Thin films of VO$_2$ were also deposited by
low-pressure CVD (LPCVD) by Sahana *et al* (2002a, 2002b),
and variation in phase transition characteristics as a function
of film microstructure were determined. Figures 5(a)–(c) show
three different implementations of the CVD technique as it has
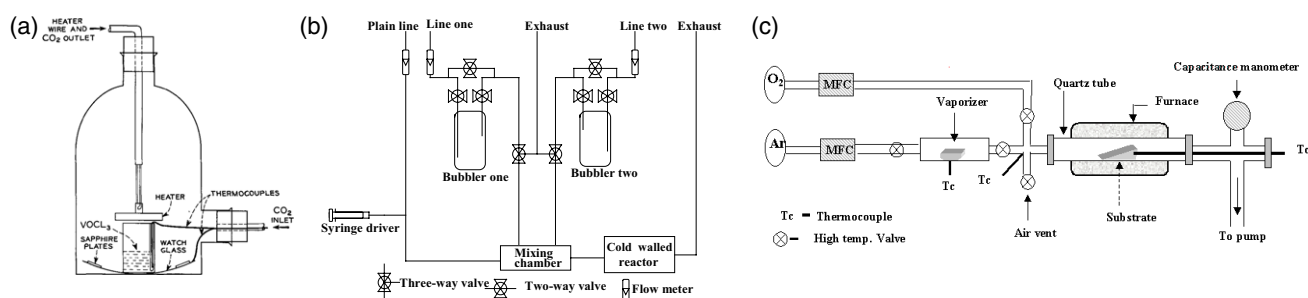evolved since the first demonstration.

Figure 5. (a) MacChesney and Guggenheim's CVD apparatus; reproduced by permission of the Electrochemical Society. (b) CVD apparatus based on VCL$_4$ and water precursors after Manning *et al* (2002). (c) Low-pressure CVD apparatus described in Sahana *et al* (2002a, 2002b). (b) and (c) reproduced by permission of the Royal Society of Chemistry.

Most recently, aerosol-assisted (AA) CVD has been demonstrated for deposition of VO$_2$ on glass (Piccirillo *et al* 2007b). In this technique, the precursor (vanadium (III) acetylacetonate and vanadyl (IV) acetylacetonate) is dispersed in a solvent and an aerosol of the solution is generated ultrasonically. The precursor is transported to the substrate through the aerosol droplets by a carrier gas. The advantage of AACVD over APCVD is that the precursor does not need to be volatile, but just soluble in a solvent suitable for aerosol formation.

4. Sol–gel method

The sol–gel method has been widely employed for depositing VO$_2$ films because of its low cost, suitability for large area deposition, and the feasibility of metal doping. The sol–gel process is a wet-chemical technique for the fabrication of materials (typically a metal oxide) starting from a chemical solution containing colloidal precursors (sol). Typical precursors are metal alkoxides and metal chlorides, which undergo hydrolysis and polycondensation reactions to form a colloid, a system composed of solid particles in sizes ranging from 1 nm to 1 μm, immersed in a solvent. The sol then evolves toward the formation of an inorganic network containing a liquid phase (gel). The formation of a metal oxide involves connecting the metal centers with oxo (M–O–M) or hydroxo (M–OH–M) bridges, thereby generating metal-oxo or metal-hydroxo polymers in solution; these polymers are then deposited on a substrate or cast in a specific container or used to synthesize powders. In the specific case of VO$_2$, the precursor is generally deposited on the desired substrate to form a film, e.g. by dip coating or spin coating. A drying process serves to remove the liquid phase, usually relatively volatile alcohols, from the gel, thus forming a porous material. A thermal annealing step is usually performed in order to favor further crystallization and enhance mechanical properties. Porosity of such films can be changed by controlling the times for annealing, but this should keep the metal–insulator transition characteristics of the film unchanged.

The sol–gel approach is a low-temperature technique that allows for the fine control on the products' chemical composition, as even small quantities of dopants, can be introduced in the sol and end up in the final product finely
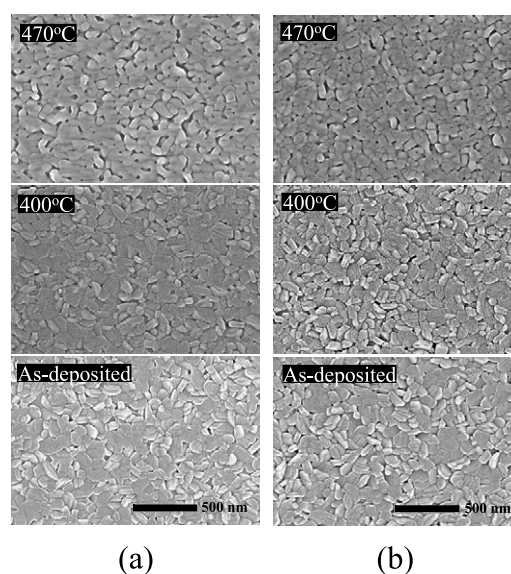

Figure 6. SEM images of vanadium oxide films grown on (a) Al$_2$O$_3$ (10$\bar{1}$2) and (b) Al$_2$O$_3$ (10$\bar{1}$0) substrates. Reprinted from Chae *et al* (2006) with permission from the Electrochemical Society.

dispersed. Thus sol–gel has been widely used to synthesize VO$_2$ doped with other metals such as tungsten or niobium to change its transition temperature. The method as applied to VO$_2$ generally consists of a spin coating with a solution of vanadium isopropoxide, VO(OC$_3$H$_7$)$_3$ diluted in an alcohol, for example, ethanol or isopropanol. This is followed by annealing in a reducing atmosphere. Greenberg introduced this process as the *gelation-hydrolysis* method for making VO$_2$ in the 1980s (Greenberg 1983). It has since been found that using the equivalent *n*-propoxide vanadium compound yields VO$_2$ also, and it is likely that a wide variety of organometallics and solvents can be used, since the final oxidation state of the vanadium ion depends on the pyrolysis conditions rather than the starting material. According to Livage *et al* (Livage 1996, 1998), vanadium oxide gels can be synthesized either via the acidification of aqueous solutions of vanadates, such as NaVO$_3$, or via the hydrolysis of vanadium oxo-alkoxides, VO(OR)$_3$. An inorganic sol–gel method using V$_2$O$_5$ as the precursor was demonstrated by Dachuan *et al* (1996). VO$_2$ films for various technological applications have been made

(a)   (b)   (c)
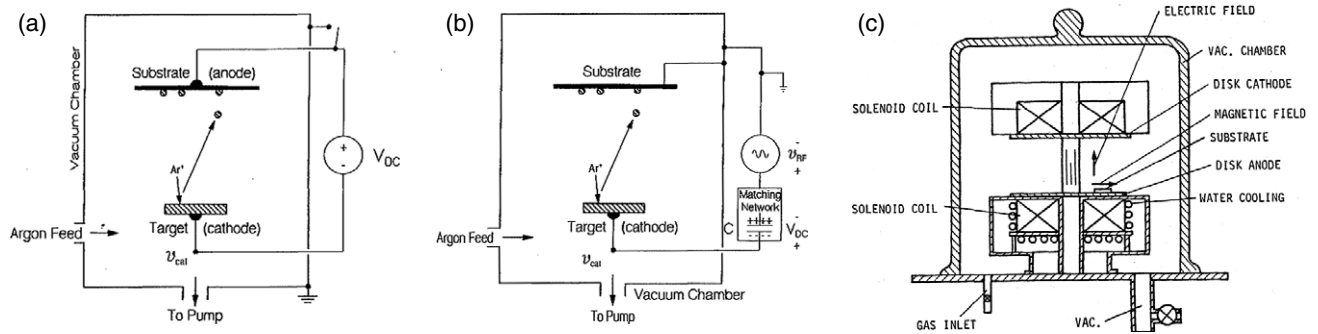

Figure 7. (a) A DC sputtering apparatus; (b) an RF sputtering apparatus; (c) a magnetron sputtering apparatus, all as described in Thornton (1983). All diagrams used by permission.

using the sol–gel process by several groups (Guzman *et al* 1995, 1996, 1994, Livage 1996, Livage *et al* 1997, Beteille and Livage 1998, Beteille *et al* 1997, Partlow *et al* 1991, Chen *et al* 2004a, 2004b, Lu *et al* 1999). Recently, Chae *et al* (2007, 2006) have developed a simplified annealing process, where using the sol–gel method they formed VO_2 followed by annealing in a low pressure of oxygen only without a reducing gas, as would otherwise be required. Typical results are shown in figure 6.

5. Sputtering

Sputtering in various forms is one of the most common physical vapor deposition processes (Thornton 1983) for growing vanadium dioxide thin films. VO_2 thin films were first grown by reactive sputtering in 1967 by Fuls, Hensler, and Ross of the Bell Telephone Laboratories (Fuls *et al* 1967), who made the films by reactive ion-beam sputtering of a vanadium target in an argon–oxygen atmosphere. The three most common methods used to facilitate the deposition process include DC, RF, and magnetron sputtering. The comparative advantages of the sputtering process include film uniformity, scalability to larger substrates, and efficiency of deposition.

The simplest form of sputtering involves a diode geometry in which energetic ions (usually argon ions) from a gas-discharge plasma bombarding a target that forms the cathode for the discharge. Target atoms bombard the substrate (the anode), forming a coating. There are three common diode sputtering arrangements, which utilize a DC discharge, a capacitative radio frequency (RF) discharge, and either a DC or a capacitative RF discharge plus a planar magnetron. Figure 7(a) shows the essential arrangement for DC sputter deposition, while figure 7(b) shows an RF sputtering arrangement with a capacitative, parallel-plate discharge, which yields substantially higher RF current. It uses a blocking capacitor to set the DC bias and an impedance-matching network for coupling to the reactive load posed by the plasma. The RF sputtering apparatus operates at lower voltage and lower sputtering gas pressures while producing higher deposition rates and, most importantly, sputtering of an electrically insulating target becomes possible (Mahan 2000, Wasa *et al* 2004).

Most contemporary high deposition-rate sources are now based on magnetron sputtering, developed in the 1970s. These sources feature a magnetically assisted argon-ion discharge, in which a permanent magnet defines lines of magnetic flux perpendicular to the applied electric field from the DC or RF source, as shown schematically in figure 7(c). The magnetic field in this arrangement is thus parallel to the surface of the target. The magnetic field concentrates and intensifies the plasma, in the space immediately above the target, by trapping of electrons near the target surface. This magnetron effect results in enhanced ion bombardment by the Ar ions, and thus much higher sputtering rates for both DC and RF discharges.

Following the first experiments in VO_2 deposition by reactive sputtering, and further analysis of those samples by Rozgonyi and Hensler (Rozgonyi and Hensler 1968, Rozgonyi and Polito 1968), both RF and DC reactive sputtering were studied by Duchene *et al* (1972). Films with similar qualities were obtained in both cases, but since RF sputtering was more suitable for depositing insulating oxides and had the above mentioned advantages over DC sputtering, it soon became the preferred method for VO_2 deposition. To standardize the fabrication of VO_2 thin films by sputter deposition, numerous studies have detailed the influence of sputter deposition parameters, such as temperature, oxygen partial pressure, plasma emission ratio of oxygen and vanadium, etc on the structural, optical, and electrical properties of the deposited VO_2. Worth mentioning amongst these are the works of Chain, Jin *et al*, Razavi *et al*, and others (Chain 1986, 1987, Guinneton *et al* 2004, Jin *et al* 1997, 1999, Jin and Tanemura 1994, Razavi *et al* 1990, 1989, Hansen and Aita 1985, Christmann *et al* 1996, Cui *et al* 1998, Dillon *et al* 2001, Mlyuka and Kivaisi 2006). Guinneton *et al* also deposited nanocrystalline VO_2 using RF sputtering (Guinneton *et al* 2001, 2000).

Inductively coupled plasma-assisted (ICP) sputtering was reported by Okimura in 2005 (Okimura and Kubo 2005, 2007) to have produced single-phase crystalline VO_2 without any residual V_2O_5 or V_3O_7. Annealing effects on VO_2 thin films deposited by reactive sputtering were also studied in detail by Fu *et al* (2006). Novel methods of making better quality VO_2 thin films by sputter deposition are being reported by groups in recent publications, showing that this is still an active area of research, which promises an even better fabrication technique for VO_2 thin films in the future (Schlag and Scherber
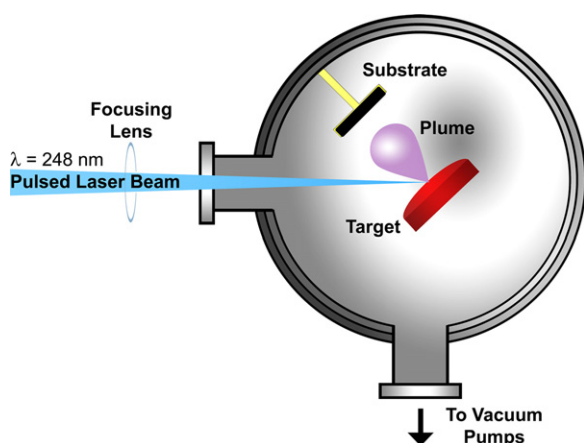
Figure 8. A typical experimental arrangement for PLD. The laser beam is scanned and the target rotated for uniform ablation.

2000). For example, Gurvitch *et al* (2007) have described a precursor oxidation process, where sputter deposited precursor V films were oxidized *in situ*, in the deposition chamber itself to produce high-quality VO_2 thin films having switching characteristics close to bulk single crystals of VO_2. VO_2 films for self-lubricating applications were produced using reactive DC magnetron sputter-ion plating physical vapor deposition (MSIP-PVD) by Lugscheider *et al* (2001).

6. Pulsed laser deposition

Pulsed laser deposition (PLD), another physical vapor deposition technique, is a comparatively recent entry into the world of thin-film depositions, and is especially suited for oxide growth. In PLD a high power pulsed laser beam is focused on a target of the desired composition inside a vacuum chamber. Material vaporized from the target is deposited as a thin film on a substrate, for example an Si wafer, facing the target. This process can occur in ultra high vacuum or in the presence of a background gas, such as oxygen which is commonly used when depositing oxides. In recent times it has become the most popular technique for VO_2 thin film and nanoparticle fabrication. Figure 8 shows the schematic diagram of a typical PLD configuration.

While the basic experimental configuration is simple compared to many other deposition techniques, the laser–target interaction phenomenology and film growth are quite complex. When the laser pulse is absorbed by the target, energy is first converted to electronic excitation and then into thermal, chemical, and mechanical energy, resulting in evaporation, ablation, plasma formation, and even exfoliation. The ejected species expand into the surrounding vacuum in the form of a plume containing many energetic species including atoms, molecules, electrons, ions, clusters, particulates, and molten globules, before depositing on substrate that is usually maintained at an elevated temperature (Chrisey and Hubler 1994, Eason 2007).

Pulsed laser ablation was developed as a deposition technique for oxide superconductors in the late 1980s, and was first used for VO_2 deposition by Singh in 1993 (Borek *et al*

1993). They employed a KrF pulsed excimer laser (248 nm) to ablate a metallic vanadium target in an ultrahigh vacuum deposition chamber with Ar and O_2 (10:1) atmosphere of 100–200 mTorr, and a substrate temperature of about ∼500 °C. The partial oxygen pressure was found to be a critical variable in favoring evolution of the pure VO_2 phase from among as many as thirteen different phases, ranging from V_4O to V_2O_5, which could exist in the system. The as-deposited samples were annealed for ∼1 h at the same temperature and pressure to obtain VO_2 films that switched when heated. Soon after, Kim and Kwok (1994) reported that they were successful in depositing high-quality VO_2 films on sapphire by PLD at high temperature *without* post-annealing. Maaza (Maaza *et al* 2000) was the first to report room-temperature growth of VO_2 by PLD without post-annealing, and the as-deposited films showed rather sharp phase transitions at around 70 °C, though it has not been reproduced by any other group yet. PLD of VO_2 thin films has been done on a variety of substrates, including silicon, glass, sapphire, fused silica, and quartz.

As noted at the beginning of this paper, Lopez *et al* were the first to make VO_2 nanocrystals by an ion-implantation method and show the size dependence of the hysteresis width during the metal–insulator transition. Other than that, VO_2 nanoparticles have been made using PLD in two different ways. In one example, a very small amount of material is deposited on a substrate and subsequently annealed to form nanoparticles of different sizes that grow by diffusion-limited aggregation and Ostwald ripening. The other way to make nanoparticles is to use lithographic patterning of a mask, using either a focused ion beam (FIB) or an electron beam, development of the mask, deposition of $VO_{1.7}$, followed by mask lift-off and annealing to produce VO_2.

In 2004, Suh *et al* (2004) described the effect of nucleation and growth of VO_2 nanoparticles and thin films on the SMT, where the films and nanoparticles were grown by PLD. They showed that the width and shape of the hysteresis cycle is determined by the competing effects of crystallinity and grain size. Figures 9 and 10 show the contrast in morphology and XRD spectra between films annealed at two different temperatures but otherwise deposited under identical conditions to a nominal thickness of 15 nm. At the higher temperature there is a substantial proportion of V_2O_5, and VO_2 created by annealing at a temperature of 550 °C rather than 450 °C. The differing morphologies and the contrasting wetting behavior of the nanoparticles suggest that, at the higher temperature, the V_2O_5 may grow as an outer layer on a VO_2 core.

In situ studies of the initial growth phase of vanadium dioxide films using synchrotron-based x-ray diffraction have been reported by the Willmott group (Pauli *et al* 2007). They showed that films grown at room temperature by reactive pulsed-gas-jet PLD are very smooth but amorphous when deposited on silicon or glass substrates, and only crystallize into the VO_2 phase upon thermal annealing in a background of O_2, forming nanoparticles that gradually agglomerate into continuous films as the deposited thickness increases. The diffraction maxima in the XRD spectra of figure 11(a) show the transition from the smooth as-grown film to the nanoparticles shown in figure 11(b).
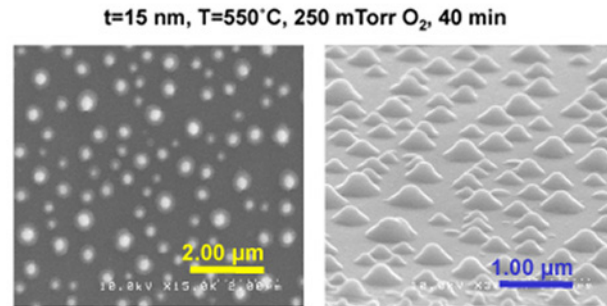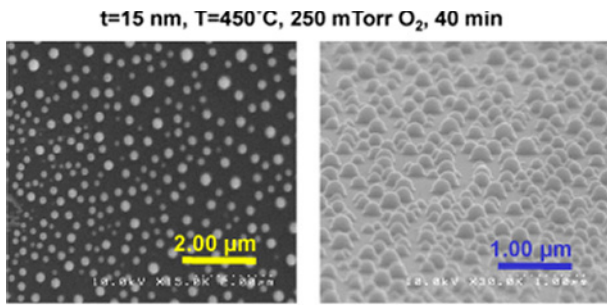
Figure 9. Contrast in nanoparticle morphology for V_xO_y films deposited under the stated conditions. Reproduced by permission of Suh *et al* 2004, copyright *J. Appl. Phys.*
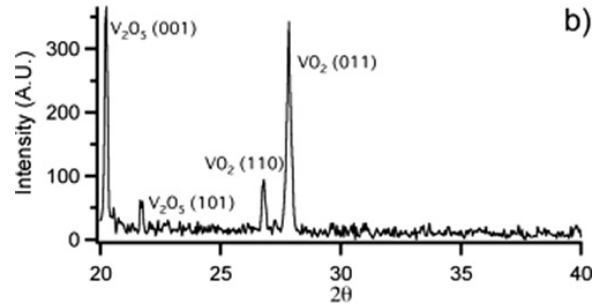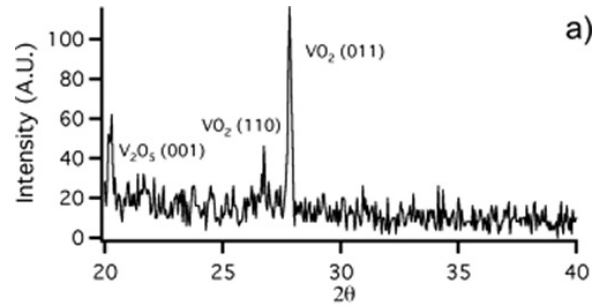

Figure 10. Comparison of XRD spectra corresponding to the upper (a) and lower (b) SEM micrographs shown in figure 9. Reproduced by permission of Suh *et al* 2004, copyright *J. Appl. Phys.*

The nano-sized VO_2 islands that form upon annealing sometimes having a preferential orientation depending on the match with the substrate crystallography. Figure 12(a) shows XRD spectra of 20 nm films of VO_2 showing spectral lines characteristic of epitaxial growth on sapphire, while figure 12(c) shows some nanoparticles that grow by Ostwald ripening when a very thin amorphous film deposited on sapphire is annealed and evidently some of them grow with preferred orientation and shape to be in conformity with the substrate lattice.

Lopez *et al* have studied the optical properties of ordered arrays of VO_2 nanoparticles, fabricated by using conventional focused ion-beam (FIB) lithography to generate a pattern in poly(methyl methacrylate), followed by a chemical lift-off process and pulsed laser deposition of $VO_{1.7}$ and a subsequent annealing in an oxygen ambient to form VO_2. When viewed by dark-field microscopy, these arrays exhibited a systematic size dependence in transition temperatures, an unusual hysteretic

response resulting from the simultaneous order–disorder and insulator-to-metal transitions, and a previously unknown optical scattering resonance in the blue spectral region (Lopez *et al* 2004b, 2004c). These unusual properties appear to result from the combination of VO_2 mesoscale optical properties and the optical coherence properties of the arrays. Figure 13 shows such an array of VO_2 nanoparticles made by FIB lithography and PLD.

Studies and manipulations of properties of films of VO_2 deposited by laser ablation are still areas of active research (Chae *et al* 2004, Soltani *et al* 2004b). More of these efforts will be discussed in detail in the epitaxy and doping sections to follow.

7. Epitaxial growth

The term epitaxy (Greek; *epi* 'above' and *taxis* 'in an ordered manner') describes ordered crystalline growth on a single-
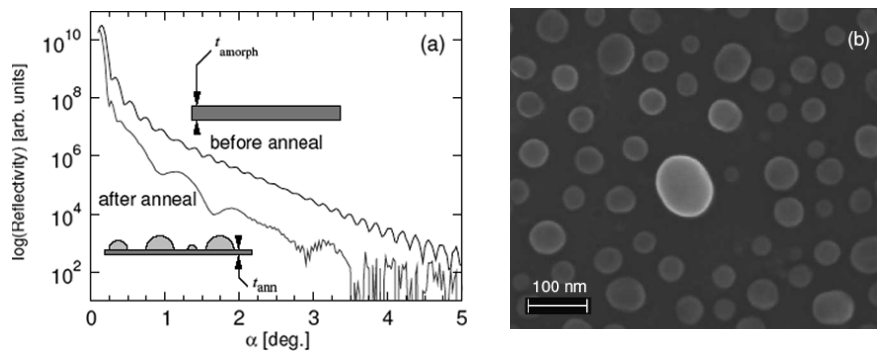

Figure 11. Characteristics of VO_2 thin films deposited by reactive gas-jet PLD on a silicon substrate. (a) X-ray reflectivity of a film as deposited and after annealing. (b) Scanning electron micrograph of the film characterized by the spectra and schematics shown in (a). Reproduced by permission of Pauli *et al* 2007, copyright *J. Appl. Phys.*
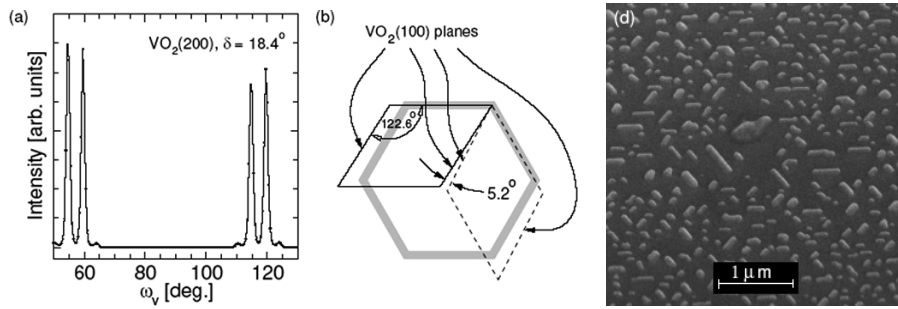
Figure 12. Characteristics of VO$_2$ thin films grown on *R*-cut sapphire substrates. (a) X-ray reflectivity spectrum of the film, showing the angular distribution characteristic of an epitaxial film. (b) Diagram showing the relationship between the lattice planes of VO$_2$ and the crystallographic axes of the sapphire. (c) Rod-like nanoparticles grown in sapphire, showing the alignment of the nanoparticles. Reproduced by permission of Pauli *et al* 2007, copyright *J. Appl. Phys.*
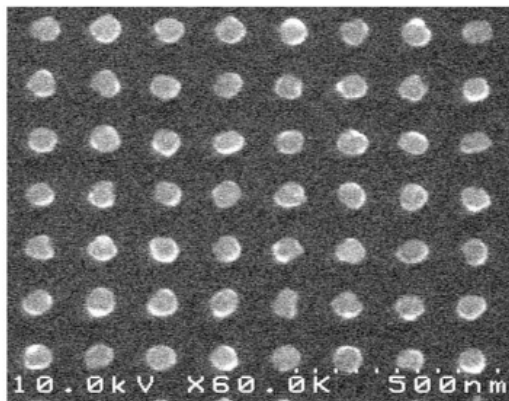

Figure 13. Section of a 100 μm × 100 μm array of VO$_2$ nanoparticles made by focused ion-beam lithography followed by pulsed laser deposition. Reproduced by permission of Lopez *et al* 2004b, copyright *Phys. Rev. Lett.*

crystalline substrate. Epitaxial films may be grown from gaseous or liquid precursors. Because the substrate acts as a seed crystal, the deposited film takes on a lattice structure and orientation identical to those of the substrate. This is different from other thin-film deposition methods which deposit polycrystalline or amorphous films, even on single-crystal substrates. If a film is deposited on a substrate of

the same composition, the process is called homoepitaxy; otherwise it is called heteroepitaxy. Homoepitaxy is frequently used for growing a film of higher purity than the substrate, and fabricating layers with different doping levels. Heteroepitaxy thus simply refers to epitaxial growth of a crystalline film on a crystalline substrate or film of another material. This technology is critical in thin-film materials science and semiconductor technology because of the need to grow crystalline films of materials of which single crystals cannot be obtained and to fabricate integrated structures composed of crystalline layers of different materials.

The substrate plays an important role in the quality of the epitaxial films and their microstructures, because of the existence of lattice mismatch—the differences from either lattice constant or angle of the lattice vectors between substrate and grown film. During epitaxy, for a few monolayers of film deposited, the lattice period of the film is changed to ensure complete matching at the interface (pseudomorphism), and for thicker films the natural lattice periods are preserved in epitaxy (commensurateness) and the differences in the periods are compensated by the appearance of misfit dislocations. Either of these happens depending on the topography and the symmetry of the substrates and deposition parameters.

Usually, the same crystallographic crystal is chosen as the substrate, as that reduces the angle deviation to zero, thereby largely reducing the lattice misfit, which is then only
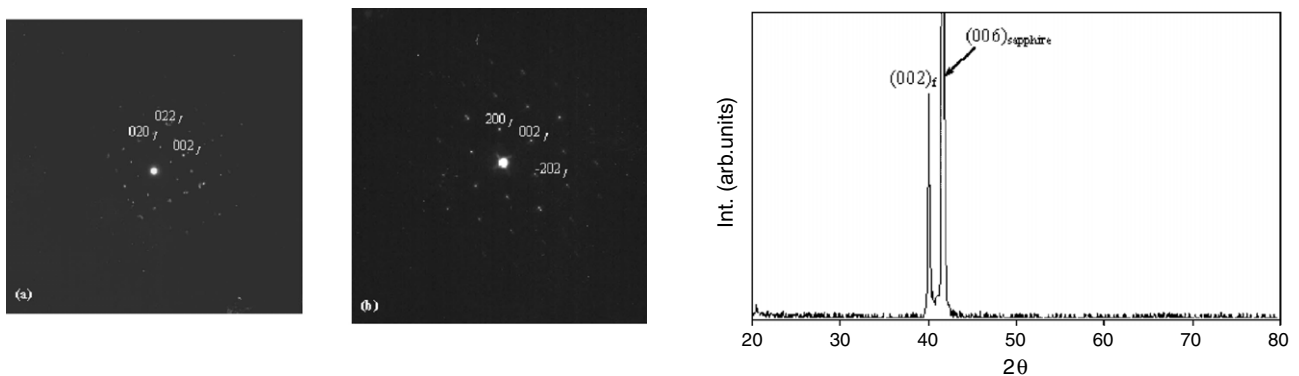

Figure 14. Characteristics of an epitaxial VO$_2$ thin film grown on sapphire. On the left, selected-area electron diffraction patterns from films grown in two different orientations. On the right, x-ray diffraction pattern from an epitaxial film grown on sapphire. Reproduced by permission of Narayan and Bhosle 2006, copyright *J. Appl. Phys.*

determined by the difference in lattice constants. But in some cases, it is hard to choose a same crystallographic crystal for the substrate, as for the monoclinic VO_2 crystal system. Difficulty also arises due to the thermal mismatch between the substrate and the films because depending on the deposition technique during the epitaxial growth the substrate could be at an elevated temperature, and more so because of the first-order phase transformation of VO_2 from the high-temperature tetragonal phase to the low-temperature monoclinic phase during the cooling process following deposition.

Sapphire, the single-crystal form of Al_2O_3, especially the R-cut plane $(01\bar{1}2)$ and the C-cut plane (0001) of Al_2O_3, because of their lattice match with VO_2 (of order 5%), as shown in table 1 even though Al_2O_3 has a hexagonal lattice while VO_2 is monoclinic, has been the preferred substrate for epitaxial growth of VO_2, since the beginning of VO_2 deposition by CVD by MacChesney *et al* (1968), and has remained so with the attempts of growing epitaxial VO_2 by different sputtering methods (Xu *et al* 2005) such as sol–gel methods (Chae *et al* 2006), PLD technique (Narayan and Bhosle 2006), and activated reactive evaporation (ARE) (Bialas *et al* 1999). It is the preferred substrate due to its easy availability, stability at high temperatures, and lower reactivity with the oxides. Figure 14 shows the characteristic structures of epi-VO_2 on sapphire.

As a matter of fact, the very first researchers (Koide and Takei 1967, Fuls *et al* 1967) to grow VO_2 thin films by CVD reported the growth of epitaxial VO_2 single-crystal films on rutile crystals having *arbitrary* surface indices. Also, Rozgonyi and Hensler in 1968 reported the growth of epitaxial VO_2 films on rutile, with reactive sputtering, and their films on sapphire were observed to be textured.

Epitaxial films of VO_2 on sapphire were deposited by reactive sputtering (Rogers *et al* 1991), followed by a demonstration of VO_2 and W-doped VO_2 epitaxial films by magnetron sputtering (Jin *et al* 1997, 1999). Singh (Borek *et al* 1993) first showed that strongly oriented and single-phase VO_2 with (200) planes parallel to the R-cut sapphire substrate can be grown using PLD, and that it exhibits a narrow transition width of 2 K, and resistivity changes of 3×10^4. Zhang (Zhang *et al* 1994) produced epitaxial VO_2 films on sapphire in 1994 using the MOCVD technique and studied the orientation relationships of substrate and film in detail. Garry *et al* (2004) attempted epitaxial growth of VO_2 on both R- and C-cut sapphire, and found that VO_2 films on R-cut planes exhibit a sharper electrical transition at a lower temperature than those deposited on C-cut planes, and optical transmission of those films also confirmed the electrical results.

In the last few years, much work has been devoted to understanding the structural properties of VO_2 on Al_2O_3, to get an insight into the mechanism of the phase transition, and this includes quite a few publications from the group of Wu and Naramoto in Japan (Wu 2000, Wu *et al* 1998, Wu and Fang 1999). Notably, in 2001, Muraoka (Muraoka and Hiroi 2002) reported epitaxial growth of VO_2 on TiO_2 (001 and 110 planes) where the lattice mismatch is ∼0.85%, and showed that the transition temperature of the deposited epitaxial VO_2 films had a strong dependence on the substrate's plane of orientation,

that is, growth conditions can affect the strain on VO_2, thereby modifying its transition properties. Also, ultrathin films of VO_2 grown epitaxially on TiO_2 by PLD were deposited by Nagashima *et al* (2006), and the effect of strain on switching properties was described.

8. Doping of VO_2 films

Transition temperatures around 67 °C for VO_2 are too high for many practical applications. Doping can lower the transition temperature, T_t, significantly, and hence doping of VO_2 has been tried extensively for a long time to make it suitable for many important applications. Dopants such as W, Ti, F, Mo, Nb, Cr, Li, and Al have been used to manipulate T_t. Earlier successful attempts at doping were made by many groups (Greenberg 1983, Goodenough 1971, Guzman *et al* 1995, Jorgenson and Lee 1986, Horlin *et al* 1972a, 1972b, 1973, 1976, Granqvist 1990). The doping process is easier in CVD and sol–gel techniques, but has also been achieved with the help of co-sputtering, and use of multiple targets or metal-doped targets in the PLD. The reported transition-temperature shifts on doping with different types of dopants has been quite significant (table 1). But, in some cases, with the decrease of T_t, the electrical and optical properties degrade as well. Refer to figure 15 for Raman spectra.

In order to understand the effects of dopants on the phase transition it is necessary to study the structural characteristics of the films before and after doping, and to find the lattice locations of the dopant atoms, that is, whether they enter the network and deliver carriers or remain in the interstitial and induce stress release or form defect centers. This was studied in epitaxially grown VO_2 by Wu *et al* (1999), where they had doped VO_2 with Mo and concluded that Mo is a substitutional dopant, which decreased T_t, and simultaneously reduced the sharpness of transitions. They concluded that since intrinsic VO_2 thin film is n-type, any acceptor doping will compensate for undoped n-type intrinsic VO_2, thereby lowering its transition temperature but still keeping its metal–insulator transition characteristics uncompromised, i.e. retaining the contrast in resistivity and reflectivity changes during the transition.

Livage (Beteille and Livage 1998) using sol–gel deposition demonstrated an extensive tailoring of the T_t and switching properties of VO_2 films by doping them with cations such as W^{6+}, Nb^{5+}, Ti^{4+}, Cr^{3+}, Al^{3+}, in varied proportions, and found that the transition temperature was reduced when doped with high-valence atoms (W^{6+}) compared to an elevated transition temperature when doped with lower valent atoms like Al^{3+}, Cr^{3+}, etc. Manning (Manning and Parkin 2004a, Manning *et al* 2005) also demonstrated successful doping of VO_2 with tungsten and other cations such as Mo and Nb using the CVD process.

It was shown by Jin *et al* (1998, 2000) initially by ion-implantation and later by magnetron sputtering, and subsequently also by Soltani *et al* (2004b) in PLD, that T_t can be reduced by W-doping in proper proportions in films. Jin *et al* (1996) also demonstrated the same thing for Mo-doping in magnetron-sputtered VO_2 films. More such efforts
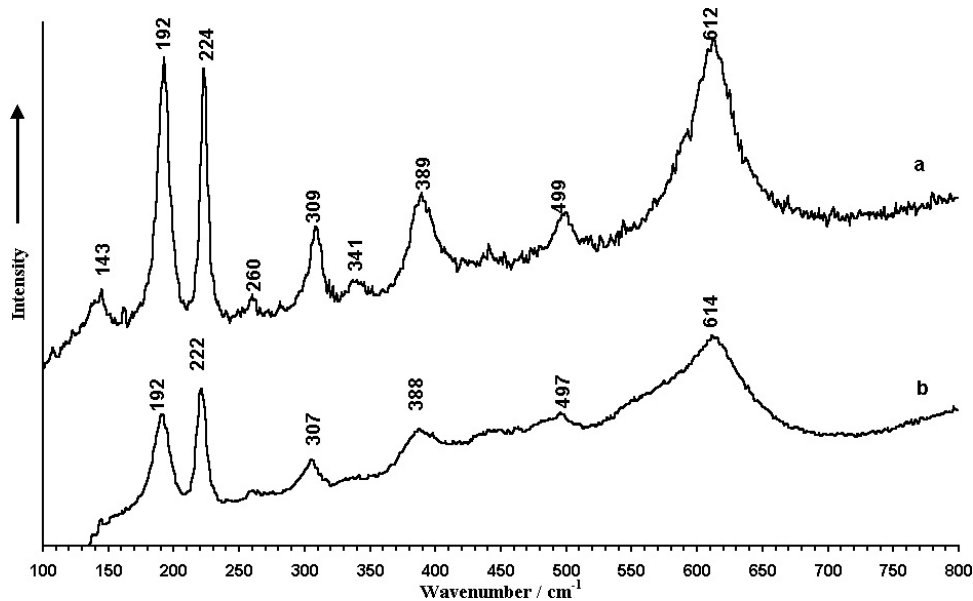
Figure 15. Raman spectra of undoped (top) and W-doped (bottom) VO_2 films using a CVD process. Reprinted with permission from Manning and Parkin (2004a, 2004b). Copyright (2004) American Chemical Society.

Table 1. The effect of doping VO_2 on the transition temperature.

Dopant	Concentration (at.%)	Transition temperature decreases by
Tungsten (W) (Jorgenson and Lee 1986)	1.0	22–28 °C
Molybdenum (Mo)	1.5 (Wu *et al* 1999), 1.0 (Jorgenson and Lee 1986)	35 °C (Wu *et al* 1999), 11 °C (Jorgenson and Lee 1986)
Niobium (Nb) (Jorgenson and Lee 1986, Guzman *et al* 1995)	1.0	8 °C

from several other research groups resulted in publications like Binions *et al* 2007, Cavanna *et al* 1999, Piccirillo *et al* 2007b, Beteille *et al* 1997, and others. Control of T_t makes these films more suitable for a wide variety of applications.

Recently, co-doping has also attempted. Burkhardt *et al* (1999, 2002) were the first to try tungsten and fluorine co-doping by sputtering; they observed that the two doping elements act independently of each other, so that their conjugated influence on phase transition is the superposition of the respective influence of each element. Takahashi *et al* (2001) investigated both W–Mo and W–Ti co-doping by the sol–gel technique, and interaction of W and Ti was found to be stronger than that between W and Mo. The advantage of W–Ti co-doping is that it permits one to control and to tailor the transition behavior, such as smoothing the gradient and reducing optical and electrical hysteresis. This was also demonstrated by Soltani *et al* (2004a). Multilayer films such as VO_2/V_2O_3 and TiO_2/VO_2 (Chang *et al* 1991) have also been successfully deposited, providing an alternative to doping as a means of controlling the temperature-dependent response and other characteristics of the films.

9. Conclusions

Thin films of vanadium dioxide have long been candidates for 'smart materials' applications ranging from memory devices to thermochromic windows. The resurgence of interest in

VO_2 as a model strongly correlated material has matched that technological interest by renewed studies of the mechanism of the metal–insulator transition and the nanoscale size dependence of these properties. Advances continue to be made in all of the classic thin-film deposition techniques, including MOCVD, sol–gel synthesis, sputtering and PLD. Optical and electrical studies of both films and nanoparticles have demonstrated that local inhomogeneities probably play crucial roles in the dynamics of phase transitions in VO_2. Since epitaxial growth improves structural homogeneity as well as electrical and optical characteristics, the objective of much current activity is directed toward higher quality, epitaxial VO_2 films with still larger optical and resistance switching contrasts. Doping and the incorporation of VO_2 films into heterostructures with tailored hysteresis characteristics and more rapid optical switching speeds will increase demand for thin-film VO_2 materials for high-performance microelectronic circuits, thermal energy management, and opto-electronic applications. Given the many opportunities represented by both the science and technology of VO_2 thin films, we can expect continuing vigorous development of the necessary deposition techniques.

Acknowledgments

References

Adler D 1968 Mechanisms for metal–nonmetal transitions in transition-metal oxides and sulfides *Rev. Mod. Phys.* **40** 714–36

Adler D and Brooks H 1967 Theory of semiconductor-to-metal transitions *Phys. Rev.* **155** 826–40

Adler D, Feinleib J, Brooks H and Paul W 1967 Semiconductor-to-metal transitions in transition-metal compounds *Phys. Rev.* **155** 851–60

Barker A S, Verleur H W and Guggenheim H J 1966 Infrared optical properties of vanadium dioxide above and below transition temperature *Phys. Rev. Lett.* **17** 1286–9

Becker M F, Buckman A B, Walser R M, Lepine T, Georges P and Brun A 1994 Femtosecond laser excitation of the semiconductor–metal phase transition in VO$_2$ *Appl. Phys. Lett.* **65** 1507–9

Berglund C N and Guggenheim H J 1969 Electronic properties of VO$_2$ near semiconductor–metal transition *Phys. Rev.* **1** 1022–33

Beteille F and Livage J 1998 Optical switching in VO$_2$ thin films *J. Sol–Gel Sci. Technol.* **13** 915–21

Beteille F, Morineau R, Livage J and Nagano M 1997 Switching properties of V$_{1-x}$Ti$_x$O$_2$ thin films deposited from alkoxides *Mater. Res. Bull.* **32** 1109–17

Bialas H, Dillenz A, Downar H and Ziemann P 1999 Epitaxial relationships and electrical properties of vanadium oxide films on r-cut sapphire *Thin Solid Films* **338** 60–9

Binions R, Piccirillo C and Parkin I P 2007 Tungsten doped vanadium dioxide thin films prepared by atmospheric pressure chemical vapour deposition from vanadyl acetylacetonate and tungsten hexachloride *Surf. Coat. Technol.* **201** 9369–72

Borek M, Qian F, Nagabushnam V and Singh R K 1993 Pulsed-laser deposition of oriented VO$_2$ thin films on *R*-cut sapphire substrates *Appl. Phys. Lett.* **63** 3288–90

Burkhardt W, Christmann T, Franke S, Kriegseis W, Meister D, Meyer B K, Niessner W, Schalch D and Scharmann A 2002 Tungsten and fluorine co-doping of VO$_2$ films *Thin Solid Films* **402** 226–31

Burkhardt W, Christmann T, Meyer B K, Niessner W, Schalch D and Scharmann A 1999 W- and F-doped VO$_2$ films studied by photoelectron spectrometry *Thin Solid Films* **345** 229–35

Case F C 1987 Influence of ion-beam parameters on the electrical and optical-properties of ion-assisted reactively evaporated vanadium dioxide thin-films *J. Vac. Sci. Technol.* A **5** 1762–6

Case F C 1991 Improved VO$_2$ thin-films for infrared switching *Appl. Opt.* **30** 4119–23

Cavalleri A, Chong H H W, Fourmaux S, Glover T E, Heimann P A, Kieffer J C, Mun B S, Padmore H A and Schoenlein R W 2004a Picosecond soft x-ray absorption measurement of the photoinduced insulator-to-metal transition in VO$_2$ *Phys. Rev.* B **69** 153106

Cavalleri A, Dekorsy T, Chong H H W, Kieffer J C and Schoenlein R W 2004b Evidence for a structurally-driven insulator-to-metal transition in VO$_2$: a view from the ultrafast timescale *Phys. Rev.* B **70** 161102

Cavalleri A, Rini M, Chong H H W, Fourmaux S, Glover T E, Heimann P A, Kieffer J C and Schoenlein R W 2005 Band-selective measurements of electron dynamics in VO$_2$ using femtosecond near-edge x-ray absorption *Phys. Rev. Lett.* **95** 067405

Cavalleri A, Rini M and Schoenlein R W 2006 Ultra-broadband femtosecond measurements of the photo-induced phase transition in VO$_2$: from the mid-IR to the hard x-rays *J. Phys. Soc. Japan* **75** 011004

Cavalleri A, Toth C, Siders C W, Squier J A, Raksi F, Forget P and Kieffer J C 2001 Femtosecond structural dynamics in VO$_2$ during an ultrafast solid–solid phase transition *Phys. Rev. Lett.* **87** 237401

Cavanna E, Segaud J P and Livage J 1999 Optical switching of Au-doped VO$_2$ sol–gel films *Mater. Res. Bull.* **34** 167–77

Chae B G, Kim H T, Yun S J, Kim B J, Lee Y W and Kang K Y 2007 Comparative analysis of VO$_2$ thin films prepared on sapphire and SiO$_2$/Si substrates by the sol–gel process *Japan. J. Appl. Phys.* 1 **46** 738–43

Chae B G, Kim H T, Yun S J, Kim B J, Lee Y W, Youn D H and Kang K Y 2006 Highly oriented VO$_2$ thin films prepared by sol–gel deposition *Electrochem. Solid State Lett.* **9** C12–4

Chae B G, Youn D H, Kim H T, Maeng S L and Kang K Y 2004 Fabrication and electrical properties of pure VO$_2$ phase films *J. Korean Phys. Soc.* **44** 884–8

Chain E E 1986 The influence of deposition temperature on the structure and optical properties of vanadium-oxide films *J. Vac. Sci. Technol.* A **4** 432–5

Chain E E 1987 Effects of oxygen in ion-beam sputter deposition of vanadium oxide *J. Vac. Sci. Technol.* A **5** 1836–9

Chang H L M, Gao Y, Guo J, Foster C M, You H, Zhang T J and Lam D J 1991 Heteroepitaxial growth of TiO$_2$, VO$_2$, and TiO$_2$/VO$_2$ multilayers by MOCVD *J. Physique* IV **1** 953–60

Chen H-K, Hung H-C, Yang T C K and Wang S-F 2004a The preparation and characterization of transparent nano-sized thermochromic VO$_2$–SiO$_2$ films from the sol–gel process *J. Non-Cryst. Solids* **347** 138–43

Chen S, Yi X, Ma H, Wang H, Tao X, Chen M and Ke C 2003 A novel structural VO$_2$ micro-optical switch *Opt. Quantum Electron.* **35** 1351–5

Chen S H, Ma H, Yi X J, Xiong T, Wang H C and Ke C J 2004b Smart VO$_2$ thin film for protection of sensitive infrared detectors from strong laser radiation *Sensors Actuators* A **115** 28–31

Chivian J S, Scott M W, Case W E and Krasutsky N J 1985 An improved scan laser with a VO$_2$ programmable mirror *IEEE J. Quantum Electron.* **21** 383–90

Chrisey D B and Hubler G K 1994 *Pulsed Laser Deposition of Thin Films* (New York: Wiley)

Christmann T, Felde B, Niessner W, Schalch D and Scharmann A 1996 Thermochromic VO$_2$ thin films studied by photoelectron spectroscopy *Thin Solid Films* **287** 134–8

Cole B E, Higashi R E and Wood R A 1998 *Proc. IEEE* **86** 1679

Cui J Z, Da D A and Jiang W S 1998 Structure characterization of vanadium oxide thin films prepared by magnetron sputtering methods *Appl. Surf. Sci.* **133** 225–9

Dachuan Y, Niankin X, Jingyu Z and Xiulin Z 1996 Vanadium dioxide films with good electrical switching property *J. Phys. D: Appl. Phys.* **29** 1051–7

Dillon R O, Le K and Ianno N 2001 Thermochromic VO$_2$ sputtered by control of a vanadium–oxygen emission ratio *Thin Solid Films* **398** 10–6

Duchene J, Terraill M and Pailly M 1972 RF and DC reactive sputtering for crystalline and amorphous VO$_2$ thin-film deposition *Thin Solid Films* **12** 231–4

Eason R (ed) 2007 *Pulsed Laser Deposition of Thin Films: Applications-Led Growth of Functional Materials* (Hoboken, NJ: Wiley-Interscience–Wiley)

Eyert V 2002 The metal–insulator transitions of VO$_2$: A band theoretical approach *Ann. Phys., Lpz* **11** 650–702

Fan J C C, Fetterman H R, Bachner F J, Zavracky P M and Parker C D 1977 Thin-film VO$_2$ submillimeter-wave modulators and polarizers *Appl. Phys. Lett.* **31** 11–3

Feldman L C and Mayer J W 1986 *Fundamentals of Surface and Thin Film Analysis* (New York: Elsevier Science)

Fu G H, Polity A, Volbers N and Meyer B K 2006 Annealing effects on VO$_2$ thin films deposited by reactive sputtering *Thin Solid Films* **515** 2519–22

Fukuma M, Zembutsu S and Miyazawa S 1982 Preparation of VO thin film and its direct optical bit recording characteristics *Appl. Opt.* **22** 265–8

Fuls E N, Hensler D H and Ross A R 1967 Reactively sputtered vanadium dioxide thin films *Appl. Phys. Lett.* **10** 199–201

Garry G, Durand O and Lordereau A 2004 Structural, electrical and optical properties of pulsed laser deposited VO_2 thin films on R- and C-sapphire planes *Thin Solid Films* **453/454** 427–30

Gea L A and Boatner L A 1996 Optical switching of coherent VO_2 precipitates formed in sapphire by ion implantation and annealing *Appl. Phys. Lett.* **68** 3081–3

Gea L A, Boatner L A, Evans H M and Zuhr R 1997 Optically active surfaces formed by ion implantation and thermal treatment *Nucl. Instrum. Methods Phys. Res.* B **127** 553–6

Golan G, Axelevitch A, Sigalov B and Gorenstein B 2003 Metal–insulator phase transition in vanadium oxides films *Microelectron. J.* **34** 255–8

Golan G, Axelevitch A, Sigalov B and Gorenstein B 2004 Investigation of phase transition mechanism in vanadium oxide thin films *J. Optoelectron. Adv. Mater.* **6** 189–95

Goodenough J B 1971 Two components of crystallographic transition in VO_2 *J. Solid State Chem.* **3** 490–500

Granqvist C G 1990 Chromogenic materials for transmittance control of large-area windows *Crit. Rev. Solid State Mater. Sci.* **16** 291–308

Greenberg C B 1983 Undoped and doped VO_2 films grown from $VO(OC_3H_7)_3$ *Thin Solid Films* **110** 73–82

Greenberg C B 1994 Optically switchable thin films—a review *Thin Solid Films* **251** 81–93

Griffith C H and Eastwood H K 1974 Influence of stoichiometry on metal–semiconductor transition in vanadium dioxide *J. Appl. Phys.* **45** 2201–6

Guinneton F, Sauques L, Valmalette J C, Cros F and Gavarri J R 2001 Comparative study between nanocrystalline powder and thin film of vanadium dioxide VO_2: electrical and infrared properties *J. Phys. Chem. Solids* **62** 1229–38

Guinneton F, Sauques L, Valmalette J C, Cros F and Gavarri J R 2004 Optimized infrared switching properties in thermochromic vanadium dioxide thin films: role of deposition process and microstructure *Thin Solid Films* **446** 287–95

Guinneton F, Valmalette J-C and Gavarri J-R 2000 Nanocrystalline vanadium dioxide: synthesis and mid-infrared properties *Opt. Mater.* **15** 111–4

Gurvitch M, Halioua M, Kastalsky A, Naar S and Shokhor S 1999 *High Speed Solid State Optical Display* ed U S P Office (USA: Copytele)

Gurvitch M, Luryi S, Polyakov A, Shabalov A, Dudley M, Wang G, Ge S and Yakovlev V 2007 VO_2 films with strong semiconductor to metal phase transition prepared by the precursor oxidation process *J. Appl. Phys.* **102** 033504

Guzman G, Beteille F, Morineau R and Livage J 1995 Thermochromic $V_{1-x}Nb_xO_2$ sol–gel thin fims *Eur. J. Solid State Inorg. Chem.* **32** 851–61

Guzman G, Beteille F, Morineau R and Livage J 1996 Electrical switching in VO_2 sol–gel films *J. Mater. Chem.* **6** 505–6

Guzman G, Morineau R and Livage J 1994 Synthesis of vanadium dioxide thin films from vanadium alkoxides *Mater. Res. Bull.* **29** 509–15

Hansen S D and Aita C R 1985 Low-temperature reactive sputter deposition of vanadium oxide *J. Vac. Sci. Technol.* A **3** 660–3

Hood P J and DeNatale J F 1991 Millimeter-wave dielectric properties of epitaxial vanadium dioxide thin films *J. Appl. Phys.* **70** 376–81

Horlin T, Kihlborg L, Niklewsk T and Nygren M 1972a Phase-transitions in doped VO_2 *Acta Crystallogr.* A **28** S174

Horlin T, Niklewsk T and Nygren M 1972b Electrical and magnetic properties of $V_{1-x}W_xO_2$, $O' = X' = 0.060$ *Mater. Res. Bull.* **7** 1515–24

Horlin T, Niklewsk T and Nygren M 1973 Magnetic, electrical and thermal studies on $V_{1-x}Mo_xO_2$ system with $0 \leqslant x \leqslant 0.20$ *Mater. Res. Bull.* **8** 179–89

Horlin T, Niklewski T and Nygren M 1976 Magnetic, electrical and thermal studies of $V_{1-x}Ti_xO_2$ ($0 \leqslant x \leqslant 0.06$) *Acta Chem. Scand. Ser.* A **30** 619–24

Jerominek H, Picard F and Vincent D 1993 Vanadium oxide films for optical switching and detection *Opt. Eng.* **32** 2092–9

Jin P, Nakao S and Tanemura S 1998 Tungsten doping into vanadium dioxide thermochromic films by high-energy ion implantation and thermal annealing *Thin Solid Films* **324** 151–8

Jin P and Tanemura S 1994 Formation and thermochromism of VO_2 films deposited by RF magnetron sputtering at low substrate temperature *Japan. J. Appl. Phys.* 1 **33** 1478–83

Jin P and Tanemura S 1996 $V_{1-x}Mo_xO_2$ thermochromic films deposited by reactive magnetron sputtering *Thin Solid Films* **282** 239–42

Jin P, Tazawa M, Ikeyama M, Tanemura S, Macak K, Wang X, Olafsson S and Helmersson U 1999 Growth and characterization of epitaxial films of tungsten-doped vanadium oxides on sapphire (110) by reactive magnetron sputtering *J. Vac. Sci. Technol.* A **17** 1817–21

Jin P, Tazawa M, Yoshimura K, Tanemura S, Macak K and Helmersson U 2000 Epitaxial growth of W-doped VO_2/V_2O_3 multilayer on alpha-Al_2O_3 (110) by reactive magnetron sputtering *Thin Solid Films* **375** 128–31

Jin P, Yoshimura K and Tanemura S 1997 Dependence of microstructure and thermochromism on substrate temperature for sputter-deposited VO_2 epitaxial films *J. Vac. Sci. Technol.* A **15** 1113–7

Jorgenson G V and Lee J C 1986 Doped vanadium oxide for optical switching fims *Sol. Energy Mater.* **14** 205–14

Kim D H and Kwok H S 1994 Pulsed laser deposition of VO_2 thin films *Appl. Phys. Lett.* **65** 3188–90

Kim H T, Chae B G, Youn D H, Maeng S L, Kim G, Kang K Y and Lim Y S 2004 Mechanism and observation of Mott transition in VO_2-based two- and three-terminal devices *New J. Phys.* **6** 19

Kim H T, Lee Y W, Kim B J, Chae B G, Yun S J, Kang K Y, Han K J, Yee K J and Lim Y S 2006 Monoclinic and correlated metal phase in VO_2 as evidence of the Mott transition: coherent phonon analysis *Phys. Rev. Lett.* **97** 266401

Kivaisi R T and Samiji M 1999 Optical and electrical properties of vanadium dioxide films prepared under optimized RF sputtering conditions *Sol. Energy Mater. Sol. Cells* **57** 141–52

Koide S and Takei H 1967 Epitaxial growth of VO_2 single crystals and their anisotropic properties in electrical resistivities *J. Phys. Soc. Japan* **22** 946–7

Kotliar G and Vollhardt D 2004 Strongly correlated materials: insights from dynamical mean-field theory *Phys. Today* **57** 53–9

Kübler C, Ehrke H, Huber R, Lopez R, Halabica A, Haglund R F and Leitenstorfer A 2007 Coherent structural dynamics and electronic correlations during an ultrafast insulator-to-metal phase transition in VO_2 *Phys. Rev. Lett.* **99** 116401

Lakes R S, Lee T, Bersie A and Wang Y C 2001 Extreme damping in composite materials with negative-stiffness inclusions *Nature* **410** 565–7

Liebsch A, Ishida H and Bihlmayer G 2005 Coulomb correlations and orbital polarization in the metal–insulator transition of VO_2 *Phys. Rev.* B **71** 085109

Livage J 1996 Sol–gel chemistry and electrochemical properties of vanadium oxide gels *Solid State Ion.* **86–88** 935–42

Livage J 1998 Optical and electrical properties of vanadium oxide films deposited from alkoxides *Bol. Soc. Esp. Ceram. Vidr.* **37** 87–92

Livage J, Guzman G, Beteille F and Davidson P 1997 Optical properties of sol–gel derived vanadium oxide films *J. Sol–Gel Sci. Technol.* **8** 857–65

Lopez R, Boatner L A, Haynes T E, Feldman L C and Haglund R F 2002a Synthesis and characterization of size-controlled vanadium dioxide nanocrystals in a fused silica matrix *J. Appl. Phys.* **92** 4031–6

Lopez R, Boatner L A, Haynes T E, Haglund R F Jr and Feldman L C 2004a Switchable reflectivity on silicon from a composite VO_2–SiO_2 protecting layer *Appl. Phys. Lett.* **85** 1410–2

Lopez R, Boatner L A, Haynes T E, Haglund R F and Feldman L C 2001 Enhanced hysteresis in the semiconductor-to-metal phase transition of VO_2 precipitates formed in SiO_2 by ion implantation *Appl. Phys. Lett.* **79** 3161–3

Lopez R, Feldman L C and Haglund R F Jr 2004b Size-dependent optical properties of VO_2 nanoparticle arrays *Phys. Rev. Lett.* **93** 177403

Lopez R, Haynes T E, Boatner L A, Feldman L C and Haglund R F 2002b Size effects in the structural phase transition of VO_2 nanoparticles *Phys. Rev.* B **65** 224113

Lopez R, Suh J Y, Feldman L C and Haglund R F Jr 2004c *Ion Beam Lithographic Fabrication of Ordered VO_2 Nanoparticle Arrays* (San Francisco, CA: Materials Research Society) pp 319–24

Lu S W, Hou L S and Gan F X 1999 Surface analysis and phase transition of gel-derived VO_2 thin films *Thin Solid Films* **353** 40–4

Lugscheider E, Knotek O, Barwulf S and Bobzin K 2001 Characteristic curves of voltage and current, phase generation of tungsten and vanadium oxides deposited by reactive d.c.-MSIP-PVD-process for self-lubricating applications *Surf. Coat. Technol.* **142–144** 137–42

Maaza M, Bouziane K, Maritz J, McLachlan D S, Swanepool R, Frigerio J M and Every M 2000 Direct production of thermochromic VO_2 thin film coatings by pulsed laser ablation *Opt. Mater.* **15** 41–5

MacChesney J B and Guggenheim H J 1969 Growth and electrical properties of vanadium dioxide single crystals containing selected impurity ions *J. Phys. Chem. Solids* **30** 225–34

MacChesney J B, Potter J F and Guggenheim H J 1968 Preparation and properties of vanadium dioxide films *J. Electrochem. Soc.* **115** 52–5

Mahan J E 2000 *Physical Vapor Deposition of Thin Films* (New York: Wiley)

Manning T D and Parkin I P 2004a Atmospheric pressure chemical vapour deposition of tungsten doped vanadium (IV) oxide from $VOCl_3$, water and WCl_6 *J. Mater. Chem.* **14** 2554–9

Manning T D and Parkin I P 2004b Vanadium (IV) oxide thin films on glass and silicon from the atmospheric pressure chemical vapour deposition reaction of $VOCl_3$ and water *Polyhedron* **23** 3087–95

Manning T D, Parkin I P, Blackman C and Qureshi U 2005 APCVD of thermochromic vanadium dioxide thin films—solid solutions $V_{2-x}M_xO_2$ (M = Mo, Nb) or composites VO_2:SnO_2 *J. Mater. Chem.* **15** 4560–6

Manning T D, Parkin I P, Clark R J H, Sheel D, Pemble M E and Vernadou D 2002 Intelligent window coatings: atmospheric pressure chemical vapour deposition of vanadium oxides *J. Mater. Chem.* **12** 2936–9

Maruyama T and Ikuta Y 1993 Vanadium dioxide thin films prepared by chemical vapor deposition from vanadium (III) acetylacetonate *J. Mater. Sci.* **28** 5073–8

Mlyuka N R and Kivaisi R T 2006 Correlation between optical, electrical and structural properties of vanadium dioxide thin films *J. Mater. Sci.* **41** 5619–24

Morin F J 1959 Oxides which show a metal-to-insulator transition at the Néel temperature *Phys. Rev. Lett.* **3** 34–6

Muraoka Y and Hiroi Z 2002 Metal–insulator transition of VO_2 thin films grown on TiO_2 (001) and (110) substrates *Appl. Phys. Lett.* **80** 583–5

Nagashima K, Yanagida T, Tanaka H and Kawai T 2006 Influence of ambient atmosphere on metal–insulator transition of strained vanadium dioxide ultrathin films *J. Appl. Phys.* **100** 063714

Narayan J and Bhosle V M 2006 Phase transition and critical issues in structure–property correlations of vanadium oxide *J. Appl. Phys.* **100** 103524

Nyberg G A and Buhrman R A 1984 Preparation and optical properties of reactively evaporated VO_2 thin films *J. Vac. Sci. Technol.* A **2** 301–2

Okimura K and Kubo N 2005 Preparation of VO_2 films with metal–insulator transition on sapphire and silicon substrates by inductively coupled plasma-assisted sputtering *Japan. J. Appl. Phys.* 2 **44** L1150–3

Okimura K and Kubo N 2007 Growth of VO_2 films with metal–insulator transition on silicon substrates in inductively coupled plasma-assisted sputtering *Thin Solid Films* **515** 4992–5

Paquet D and Lerouxhugon P 1980 Electron correlations and electron–lattice interactions in the metal–insulator, ferroelastic transition in VO_2—a thermodynamical study *Phys. Rev.* B **22** 5284–301

Partlow D P, Gurkovich S R, Radford K C and Denes L J 1991 Switchable vanadium-oxide films by a sol–gel process *J. Appl. Phys.* **70** 443–52

Pauli S A, Herger R, Willmott P R, Donev E U, Suh J Y and Haglund R F Jr 2007 X-ray diffraction studies of the growth of vanadium dioxide nanoparticles *J. Appl. Phys.* **102** 073527

Piccirillo C, Binions R and Parkin I P 2007a Synthesis and functional properties of vanadium oxides: V_2O_3, VO_2, and V_2O_5 deposited on glass by aerosol-assisted CVD *Chem. Vapor Depos.* **13** 145–51

Piccirillo C, Binions R and Parkin I P 2007b Nb-doped VO_2 thin films prepared by aerosol-assisted chemical vapour deposition *Eur. J. Inorg. Chem.* **25** 4050–5

Radford W A, Murphy D F, Ray M, Propst S H, Kennedy A, Kojiro J K, Woolaway Ii J T, Soch K L, Coda R, Lung G, Moody E A, Gleichman D and Baur S T 1996 320 × 240 silicon microbolometer uncooled IR FPAs with on-chip offset correction *Infrared Detectors and Focal Plane Arrays IV* (Orlando, FL: SPIE) pp 82–92

Rajendra Kumar R T, Karunagaran B, Mangalaraj D, Narayandass S K, Manoravi P, Joseph M and Gopal V 2003 Pulsed laser deposited vanadium oxide thin films for uncooled infrared detectors *Sensors Actuators* A **107** 62–7

Razavi A, Bobyak L and Fallon P 1990 The effects of biasing and annealing on the optical properties of radiofrequency sputtered VO_2 *J. Vac. Sci. Technol.* A **8** 1391–4

Razavi A, Hughes T, Antinovitch J and Hoffman J 1989 Temperature effects on structure and optical properties of radio-frequency sputtered VO_2 *J. Vac. Sci. Technol.* A **7** 1310–3

Rini M, Cavalleri A, Schoenlein R W, López R, Feldman L C, Haglund J R F, Boatner L A and Haynes T E 2005 Photoinduced phase transition in VO_2 nanocrystals: ultrafast control of surface-plasmon resonance *Opt. Lett.* **30** 558–60

Roach W R 1971 Holographic Storage in VO_2 *Appl. Phys. Lett.* **19** 453–5

Rogers K D, Coath J A and Lovell M C 1991 Characterization of epitaxially grown films of vanadium-oxides *J. Appl. Phys.* **70** 1412–5

Rozgonyi G A and Hensler D H 1968 Structural and electrical properties of vanadium dioxide thin films *J. Vac. Sci. Technol.* **5** 194–9

Rozgonyi G A and Polito W J 1968 Preparation of thin films of vanadium (di-, sesqui- and pent-) oxide *J. Electrochem. Soc.* **115** 56–7

Ryabova L A 1981 *Current Topics in Materials Science* vol 7 (Amsterdam: North Holland)

Ryabova L A, Serbinov I A and Darevsky A S 1972 Preparation and properties of pyrolysis of vanadium-oxide films *J. Electrochem. Soc.* **119** 427–9

Sahana M B, Subbanna G N and Shivashankar S A 2002a Phase transformation and semiconductor–metal transition in thin films of VO_2 deposited by low-pressure metalorganic chemical vapor deposition *J. Appl. Phys.* **92** 6495–504

13

Sahana M B, Dharmaprakash M S and Shivashankar S A 2002b Microstructure and properties of VO$_2$ thin films deposited by MOCVD from vanadyl acetylacetonate *J. Mater. Chem.* **12** 333–8

Schlag H J and Scherber W 2000 New sputter process for VO$_2$ thin films and examination with MIS-elements and *C–V*-measurements *Thin Solid Films* **366** 28–31

Schwingenschlogl U and Eyert V 2004 The vanadium Magneli phases V$_{(n)}$O$_{(2n-1)}$ *Ann. Phys.* **13** 475–510

Sobhan M A, Kivaisi R T, Stjerna B and Granqvist C G 1996 Thermochromism of sputter deposited W$_x$V$_{1-x}$O$_2$ films *0xmne Sol. Energy Mater. Sol. Cells* **44** 451–5

Soltani M, Chaker M, Haddad E and Kruzelesky R V 2006 Thermochromic vanadium dioxide smart coatings grown on Kapton substrates by reactive pulsed laser deposition *J. Vac. Sci. Technol.* A **24** 612–7

Soltani M, Chaker M, Haddad E, Kruzelecky R and Margot J 2007 Micro-optical switch device based on semiconductor-to-metallic phase transition characteristics of W-doped VO$_2$ smart coatings *J. Vac. Sci. Technol.* A **25** 971–5

Soltani M, Chaker M, Haddad E, Kruzelecky R V and Margot J 2004a Effects of Ti–W codoping on the optical and electrical switching of vanadium dioxide thin films grown by a reactive pulsed laser deposition *Appl. Phys. Lett.* **85** 1958–60

Soltani M, Chaker M, Haddad E, Kruzelecky R V and Nikanpour D 2004b Optical switching of vanadium dioxide thin films deposited by reactive pulsed laser deposition *J. Vac. Sci. Technol.* A **22** 859–64

Suh J Y, Lopez R, Feldman L C and Haglund R F Jr 2004 Semiconductor to metal phase transition in the nucleation and growth of VO$_2$ nanoparticles and thin films *J. Appl. Phys.* **96** 1209–13

Takahashi I, Hibino M and Kudo T 2001 Thermochromic properties of double-doped VO$_2$ thin films prepared by a wet coating method using polyvanadate-based sols containing W and Mo or W and Ti *Japan. J. Appl. Phys.* 1 **40** 1391–5

Takei H and Koide S 1966 Growth and electrical properties of vanadium-oxide single crystals by oxychloride decomposition method *J. Phys. Soc. Japan* **21** 1010

Thornton J A 1983 Plasma-assisted deposition processes—theory, mechanisms and applications *Thin Solid Films* **107** 3–19

Verleur H W, Barker A S and Berglund C N 1968 Optical properties of VO$_2$ between 0.25 and 5 eV *Phys. Rev.* **172** 788–98

Walden R H 1970 Two switching devices utilizing VO$_2$ *IEEE Trans. Electron Devices* **17** 603–12

Wasa K, Kitabatake M and Adachi H 2004 *Thin Films Materials Technology* (New York: William Andrew)

Wu Z P 2000 *Defects and Diffusion in Ceramics* (Uetikon-Zuerich: Scitec Publications) pp 137–43

Wu Z P and Fang P A 1999 Epitaxial growth and phase transition properties of vanadium dioxide thin film on sapphire substrate *J. Inorg. Mater.* **14** 823–7

Wu Z P, Miyashita A, Yamamoto S, Abe H, Nashiyama I, Narumi K and Naramoto H 1999 Molybdenum substitutional doping and its effects on phase transition properties in single crystalline vanadium dioxide thin film *J. Appl. Phys.* **86** 5311–3

Wu Z P, Miyashita A, Yamamoto S, Nashiyama I, Narumi K and Naramoto H 2000 Optical properties of vanadium dioxide thin film as a windows thermochromic coating *Mater. Construct.* **50** 5–10

Wu Z P, Yamamoto S, Miyashita A, Zhang Z J, Narumi K and Naramoto H 1998 Single-crystalline epitaxy and twinned structure of vanadium dioxide thin film on (0001) sapphire *J. Phys.: Condens. Matter* **10** L765–71

Wyckoff R W G 1965 *Crystal Structures* (New York: Wiley)

Xu G, Jin P, Tazawa M and Yoshimura K 2005 Thickness dependence of optical properties of VO$_2$ thin films epitaxially grown on sapphire (0001) *Appl. Surf. Sci.* **244** 449–52

Zhang H, Chang H L M, Guo J and Zhang T J 1994 Microstructure of epitaxial VO$_2$ thin films deposited on (11$\bar{2}$) sapphire by MOCVD *J. Mater. Res.* **9** 2264–71